Journal of Advanced Research in Fluid Mechanics and Thermal Sciences

Journal homepage:
https://semarakilmu.com.my/journals/index.php/fluid_mechanics_thermal_sciences/index
ISSN: 2289-7879

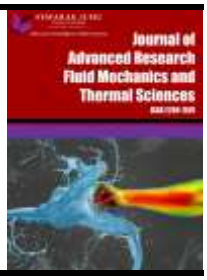

Observation of Deformation Process of Elastic Tubes for Pulsatile Flows by Impinging Jet Flows and Its Application to Novel Measurement Method of Blood Pressure

Ayumu Yamamoto[1], Yoshiki Yanagita[1], Yuko Miyamura[1,2], Takeshi Tachibana[3], Yohji Yamamoto[3], Tetsuya Kimura[4], Masaaki Tamagawa[1,*]

[1] Graduate School of Life Science and System Engineering, Kyushu Institute of Technology, Hibikino 2-4, Wakamatsu-ku, Kitakyushu, Fukuoka 808-0196, Japan
[2] Department of Nursing, Faculty of Fukuoka Medical Technology Teikyo University, Misaki-machi 6-22, Omuta, Fukuoka 836-8505, Japan
[3] Department of Mechanical Engineering, National Institute of Technology, Kitakyushu Collage, Shii 5-20-1, Kokurakita-ku, Kitakyushu, Fukuoka 802-0985, Japan
[4] Graduate School of Human Development and Environment, Kobe University, Tsurukabuto 3-11, Nada-ku, Kobe, Hyogo, Japan

ARTICLE INFO

Article history:
Received 5 April 2024
Received in revised form 30 June 2024
Accepted 12 July 2024
Available online 30 July 2024

Keywords:
Pressure measurement; pulsatile flow; impinging jet flow; deformation of elastic tube; Tonometry method

ABSTRACT

Recently, due to the spreading of COVID-19 infection, non-contact measurement of vital information has been required at hospitals. Conversely, as for the measurement of continuous blood pressure and its fluctuations, it has been more important to find a high risk of diseases earlier. Although most of them are obtained by a mechanical contact sensor based on principle of tonometry, the method cannot be applied to non-contact measurement. In this research, a novel method composed of a jet flow and a camera for measuring blood pressure without contact is proposed, and continuous blood pressure and its fluctuations can be detected by this method. In this paper, to develop this novel method, a blood arterial is simulated as an elastic tube, and the deformation process of the elastic tube is observed under pulsatile flow, and the relationship between the deformation process and blood pressure will be obtained. In the experiments, a silicone tube is used to simulate a blood vessel, and the fluid is circulated by a roller pump to create a pulsatile flow. The jet flow is targeted to the tube surface from a nozzle from 0 to 0.37 MPa, and internal pressure in the tube is measured by a pressure sensor. As a result, the displacement and the internal pressure of the tube increased rapidly when a jet flow of a certain pressure was targeted to the tube surface. In addition, it was confirmed that a gradient of cross-sectional area of the tube with the jet pressure reached to inflection point when the internal pressure increased rapidly. Therefore, there is a possibility that jet pressure applicable to blood pressure measurement can be estimated from the gradient change of the cross-sectional area.

* *Corresponding author.*
E-mail address: tama@life.kyutech.ac.jp

https://doi.org/10.37934/arfmts.119.2.149159

1. Introduction

Recently, due to the spreading of COVID-19 infection, non-contact measurement of vital information such as body temperature, blood pressure, blood oxygenation level or heart rate has been required at hospitals and nursing facilities. In general, the oscillometric method and Korotkoff method have been applied to the sphygmomanometer [1-7]. These are methods to measure diastolic blood pressure (DBP) and systolic blood pressure (SBP) during the decompression after the blood vessels are compressed with a cuff attached to the upper arm. These methods cannot be applied to continuous measurement because only temporary or intermittent DBP and SBP can be obtained due to long measuring times. Conversely, photoplethysmography (PPG) and electrocardiogram (ECG) have been applied to wearable devices, where the blood pressure is estimated by data science based on temporal information such as pulse wave propagation time (PPT) and pulse contours [8-14]. However, while DBP and SBP per beat can be obtained from the device, it is inability to ascertain rapid fluctuations in blood pressure that are valid for disease diagnosis. In addition, because skin must be attached to a light source and an electrode of the device, these methods cannot be applied to non-contact measurements. Although the application of cameras has also been studied as the non-contact measurement method, only estimated values of blood pressure based on PPT can be obtained [15]. Thus, it has been difficult to measure absolute values of blood pressure. In this current situation, it is necessary to develop a novel sensor device which can measure blood pressure directly.

As the method of continuous and direct measurement, the tonometry method has recently garnered significant attraction [16-20]. In this method, the fluctuations in blood pressure can be measured directly without measuring DBP and SBP. However, the proposed methods cannot be applied to the non-contact measurement because the piezo sensor and skin must be in contact. The purpose of this research is to develop a novel non-contact measurement system of blood pressure based on the tonometry method which can capture the fluctuations in blood pressure by using a jet flow and a camera instead of piezo sensors. First, in this paper, an experimental system which targets the jet flow at a pulsating blood vessel simulated by an elastic is developed. Second, the relationship between the deformation of the elastic tube and its internal pressure when compressed by the jet flow is investigated through observation and pressure measurement.

2. Theory of Tonometry Method

Figure 1 shows schematic of balance of forces in a radial artery when the thickness of the vessel wall is taken into account. As shown in Figure 1(a), the balance of forces at the vessel wall is expressed by Laplace law when blood vessels are not deformed by external pressure [16]

$$T=p_{\mathrm{i}}r_{\mathrm{i}}-p_{\mathrm{o}}r_{\mathrm{o}}, \tag{1}$$

where T is surface tension at the vessel wall, p_{i} is internal pressure, p_{o} is external pressure, r_{i} is radius of curvature of the inner wall of a blood vessel and r_{o} is radius of curvature of the outer wall of the blood vessel. Eq. (1) is transformed as follows

$$p_{\mathrm{i}}=\frac{r_{\mathrm{o}}}{r_{\mathrm{i}}}p_{\mathrm{o}}+\frac{T}{r_{\mathrm{i}}}. \tag{2}$$

As shown in Figure 1(b), when the blood vessel is pressed flat by external pressure, the radius of curvature of the inner wall and outer wall are $r_{\mathrm{i}} \to \infty$ and $r_{\mathrm{o}} \to \infty$, respectively. Thus, the relationship between r_{i} and r_{o} is as follows

$r_i = r_o$. (3)

Therefore, the surface tension at the blood vessel can be ignored and following equation is obtained

$p_i \approx p_o$. (4)

Eq. (4) expresses that the internal pressure is equal to the external pressure when the blood vessel is pressed flat. In the tonometry method, the radial artery is compressed flat by a known external pressure to estimate the internal pressure of the artery. Figure 2 shows the conceptual diagram of pressurization by jet flow. In this research, the internal pressure is estimated by pressing flat the radial artery with a jet flow of a known pressure as shown in Figure 2.

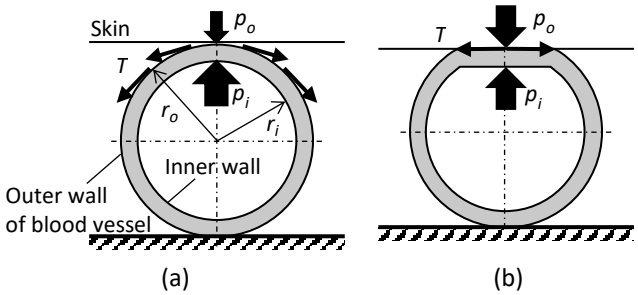

Fig. 1. Schematic of deformation of radial artery; (a) Before deformation, (b) Deformed into flat shape

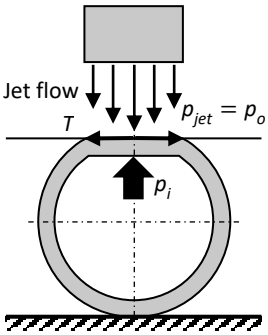

Fig. 2. Deformed into flattened by jet

3. Experimental Setup

Figure 3 shows the schematic of experimental setup developed from this research. In this experiment, the silicone tube (outer diameter 2.4 mm, inter diameter 2 mm) is used to simulate blood vessel, and the roller pump (rotation speed 60 rpm) is used to circulate water pulsatile. The air delivered from the compressor is controlled by the solenoid valve, and jets toward the silicone tube with the nozzle (inter diameter 1.7 mm). Since the control circuit including the microcomputer is connected to the solenoid valve, the jet flow is targeted synchronously with rotation of the roller pump. Figure 4 shows the solenoid valve operation process by the control circuit. From Fig. 4, the optical sensor (Omron, E3X-SD21) outputs a rotation pulse and transmits the pulse to the microcomputer when the rotator of the roller pump is detected. The microcomputer outputs a jet pulse at an arbitrary time in response to the rise of the rotation pulse, and opens the solenoid valve by activating the relay. Figure 5 shows the side view of the observation area in Figure 3. As shown in

Figure 5, the nozzle directly fixed to the solenoid valve is positioned at a horizontal distance of 1 mm from the tube surface. The deformation behavior of the tube is observed by the stereo microscope (Nikon, SMZ800) from z-axis, and filmed by the video camera (Panasonic, HDC-HS9, framerate 30 fps, shutter speed 1/8000 s) installed on the microscope. As shown in Figure 6, in this research, the maximum displacement of one side of the tube is obtained by image analysis. In addition, the internal pressure of the tube is measured by the pressure sensor (SMC, PSE573) to compare with the tube displacement, and recorded by the oscilloscope (Yokogawa Test & Measurement, DL1640, sampling rate 1 kHz) along with the rotation pulse and the jet pulse. In this experiment, the air filling pressure by the compressor is monitored by the indicator (SMC, ISE40A), and this pressure is defined as the jet pressure and set to be from 0 MPa (no jet) to 0.37 MPa. Figure 7 shows the time chart of the rotation pulse and the jet pulse. As shown in Figure 7, the number of jets per rotation of the roller pump is one, and the solenoid valve is set to be opened for 120 ms at a time 300 ms after the rise of the rotation pulse.

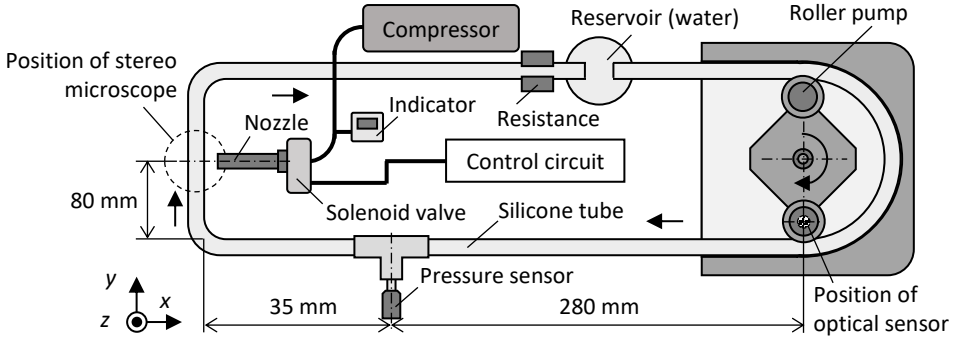

Fig. 3. Schematic of experimental setup

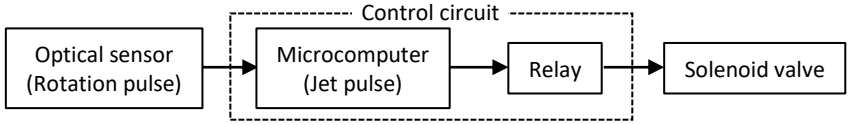

Fig. 4. Solenoid valve operation process by microcomputer

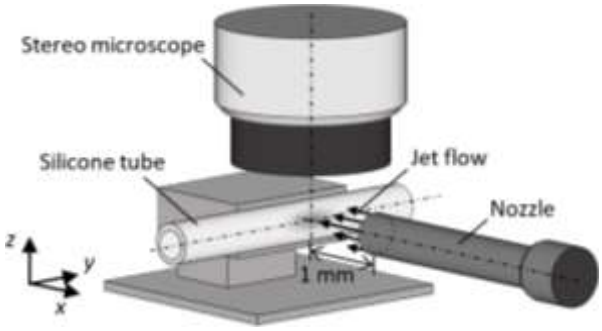

Fig. 5. Schematic of observation area

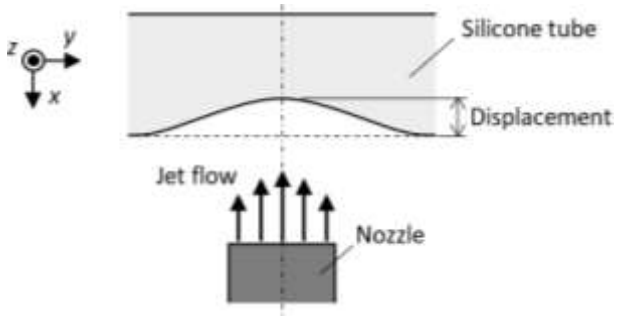

Fig. 6. Schematic of deformation of tube by jet

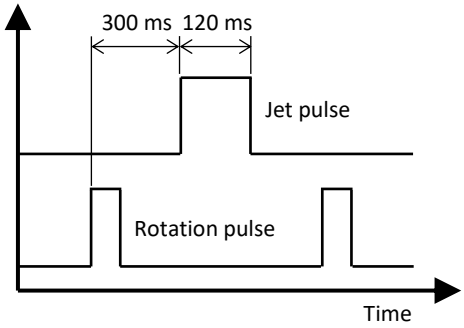

Fig. 7. Time chart for rotation pulse and jet pulse

4. Result and Discussion

4.1 Measurement of Pressure History of Jet Flow

First, pressure measurement as a preliminary experiment is conducted to understand the actual pressure of the jet flow reaching the tube surface. Figure 8 shows schematic of setup measurement jet pressure. As shown in Figure 8, the position of the pressure sensor (PCB Piezotronics, 113B24) is horizontally 1 mm from the nozzle. Figure 9 shows the pressure history at the jet pressure of 0.37 MPa as a typical result. From Figure 9, the measurement pressure raised rapidly with the time after the rise of the jet pulse represents the opening of the solenoid valve, and reached peak pressure of 116 kPa. Conversely, the measurement pressure decreased slowly after reaching peak pressure, because low-frequency response of the PCB sensor is 0.005 Hz by the specification. Thus, it is expected that the real fall time may be shorter than the result. In addition, from Figure 9(b), it is confirmed that there was a 20 ms delay between the rise of the jet pulse and the rise of measurement pressure. Conversely, since the open time of the solenoid valve is set to 120 ms as stated above, the pressure from the rise to 120 ms is considered important. Next, the averaged pressure from the rise to 120 ms was obtained at each jet pressure. Figure 10 shows the averaged pressure between the rise of the pressure and 120 ms. In Figure 10, the error bar shows 95 % confidence interval calculated from 3 measurements at each jet pressure. From Figure 10, the measurement pressure increases linearly with increasing the jet pressure. In addition, the measurement pressure is lower than the jet pressure at each condition, it is confirmed that measurement pressure reduced 10 % to 20 % of the jet pressure.

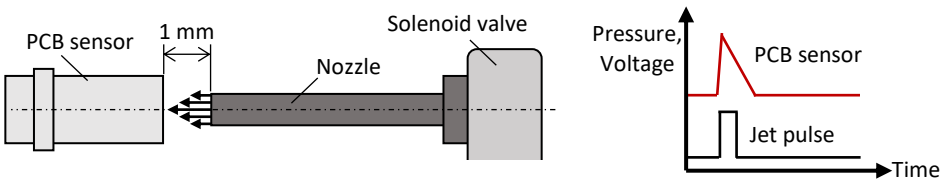

(a) Position of PCB sensor and solenoid valve (b) Schematic of output signal

Fig. 8. Schematic of measurement of actual jet pressure by PCB sensor

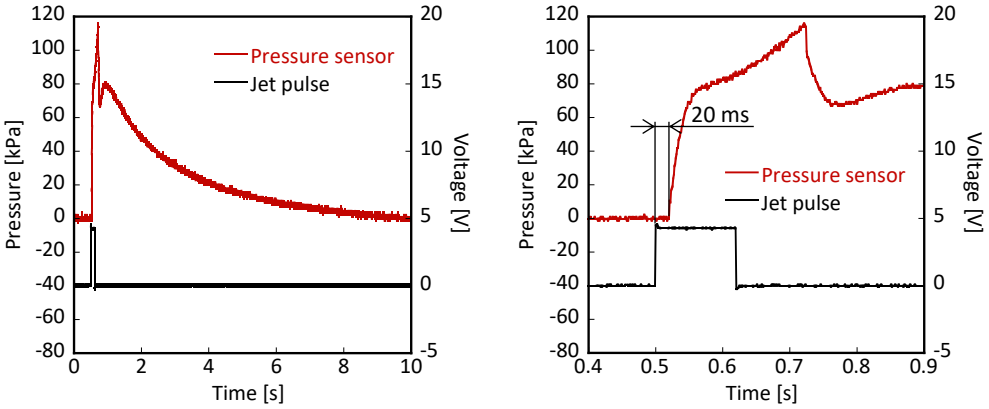

(a) Overall view (b) Enlarged view

Fig. 9. Pressure history at jet pressure for 0.37 MPa

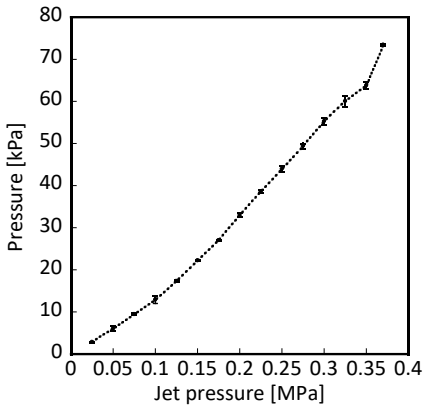

Fig. 10. Relationship between jet pressure and averaged pressure over 120 ms (error bar shows 95 % confidence interval)

4.2 Deformation and Internal Pressure Change of Elastic Tube

Figure 11 shows the time history of rotation pulse, jet pulse, displacement and internal pressure of the tube at the jet pressure of 0 MPa, 0.2 MPa and 0.37 MPa as typical results. The results were obtained from 2 periods of the rotation from the start of measurement. First, from Figure 11(a), it is observed that the pulsatile flow was generated and the internal pressure changes from 15 kPa to 20 kPa in the case of no jet flow. From this result, it is confirmed that pulsating blood vessel can be simulated by using the elastic tube and the roller pump. Next, the effects of the jet flow on deformation and the internal pressure of the tube are discussed. From Figure 11(b), the tube is slightly deformed immediately after the rise of the jet pulse when the jet pressure is 0.2 MPa. However, even when the jet flow of 0.2 MPa was targeted to the tube surface, the behavior of the internal pressure was the almost same as 0 MPa. Focusing on the case of high-jet pressure, an increase of the internal pressure was observed at the same time as the time when the tube deformation was observed in the case of increasing the jet pressure to 0.37 MPa (Figure 11(c)).

Figure 12 shows the comparison of internal pressure and displacement of the tube at each jet pressure. First, in Figure 12, averaged value of each measurement result for 120 ms (open time of solenoid valve) was obtained with a delay of 20 ms based on the rise of the jet pulse. Second, each measurement results were averaged for 5 periods of pulsatile flow. From Figure 12, it is observed

that the internal pressure increased slowly with increasing jet pressure from 0 MPa to 0.25 MPa. As shown in Figure 10, when the jet pressure is set from 0 MPa to 0.2 MPa, the actual pressure is from 10 kPa to 30 kPa at the tube surface which is close to the internal pressure in the case of no jet flow. Thus, it is considered that the slight effect of the jet flow on the internal pressure was observed. Subsequently, the internal pressure increased rapidly at jet pressures higher than 0.25 MPa. It is considered that the internal pressure changed significantly because the actual tube received pressure was 43 kPa or more which is about twice the original internal pressure (15 kPa to 20 kPa) in the case of jet pressure of 0.25 MPa (Figure 10). Therefore, it is confirmed that the jet flow affects the internal pressure of the tube when the jet pressure exceeds a certain level. However, if the blood pressure is changed by the jet flow, actual blood pressure cannot be measured, and the jet flow cannot apply to a sphygmomanometer. From this reason, the jet pressure higher than 0.25 MPa is considered excessive, and there is a possibility that the measurable range is the jet pressure lower than 0.25 MPa in this experimental system.

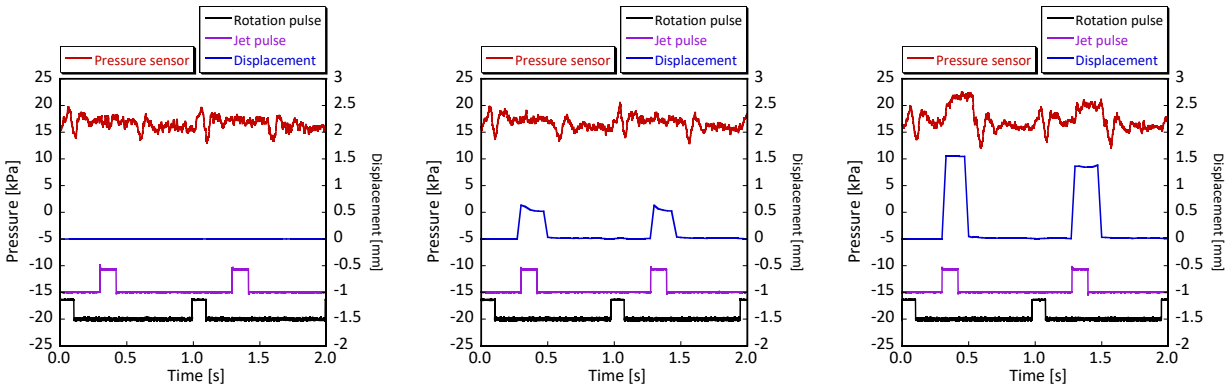

(a) Without jet flow 0 MPa (d) Jet pressure 0.2 MPa (c) Jet pressure 0.37 MPa

Fig. 11. Pressure history of rotation pulse, jet pulse, displacement of tube and internal pressure

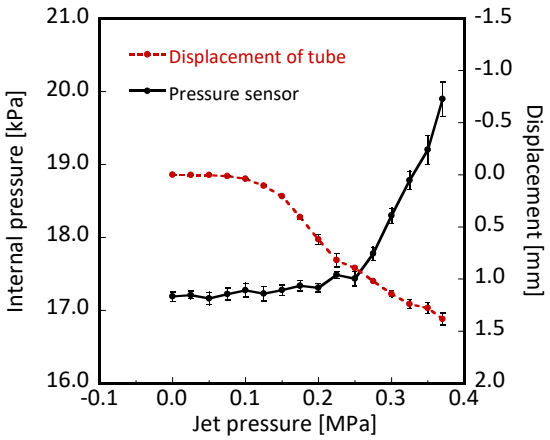

Fig. 12. Comparison of internal pressure and displacement of tube (error bar shows 95 % confidence interval)

Conversely, a significant change in the displacement of the tube was not observed at the jet pressure from 0 MPa to 0.1 MPa. However, the displacement increased linearly at the jet pressure from 0.15 MPa to 0.37 MPa. From the comparison between the internal pressure change and the displacement change, it is found that the sensitivity of the displacement changes to increasing jet pressure is higher than the internal pressure change. Since the internal pressure changes in

proportion to volume change of the tube by receiving the jet flow, it is considered that the displacement which is one-dimensional data was more sensitive than volume as three-dimensional data. However, it is difficult to capture the volume change with precision in this experiment.

Thus, the cross-sectional area of the tube is estimated from its displacement, and compared with the internal pressure. In addition, to investigate the inflection point of the area change with increasing jet pressure, the following approximate curve is applied

$$f(x)=\frac{\alpha}{1+e^{-k(x-x_0)}}+y_0, \tag{5}$$

Figure 13 shows the schematic of cross-sectional area. On the assumption that the circumference of the tube does not change before and after deformation, the cross-sectional area under pressure is calculated as elliptically varying (Figure 13(b)). The circumference of an ellipse can be calculated by following the equation

$$L=\pi\left\{3(a+b)-\sqrt{(a+3b)(3a+b)}\right\}, \tag{6}$$

where a is length of major axis and b is length of minor axis. The length of the minor axis can be calculated from the difference between the original tube diameter and the displacement obtained from image analysis. From Eq. (6), the length of the major axis is expressed as follows

$$a=\sqrt{\left\{-b^2+b\frac{l}{\pi}-\frac{1}{6}\left(\frac{L}{\pi}\right)^2+\left(\frac{2}{3}b-\frac{L}{2\pi}\right)^2\right\}}-\left(\frac{2}{3}b-\frac{L}{2\pi}\right). \tag{7}$$

The cross-sectional area is calculated as the area of the ellipse by following equation

$$S=\pi ab. \tag{8}$$

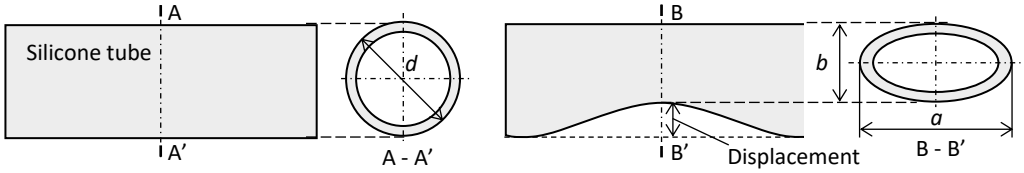

(a) Original geometry (b) Deformation under pressure

Fig. 13. Schematic of cross-sectional area change of tube

Figure 14 shows relationship between jet pressure and cross-sectional area, and approximate curve. From Figure 14, the change in the cross-sectional area is not observed at the jet pressure from 0 MPa to 0.1 MPa. Conversely, when the jet pressure is higher than 0.15 MPa, the cross-sectional area decreases significantly and linearly with increasing jet pressure. Here, the change in cross-sectional area is compared to the displacement change with increasing jet pressure. Although the displacement changed significantly at 0.1 MPa, the cross-sectional area changed at 0.15 MPa. Thus, the sensitivity of deformation with increasing the jet pressure was lowered by calculating the cross-sectional area. In Figure 14, the approximate curve is written by the dotted line. By fitting the approximate curve to the cross-sectional area, the coefficients were determined to be α = -1.817, k = 22.74, x_0 = 0.2607, y_0 = 4.524, respectively, and coefficient of determination was obtained to be R2 = 0.9997. Next, the inflection points of the area change with increasing jet pressure is investigated in detail with the approximate curve. Figure 15 shows the relationship between jet pressure and

gradient of the cross-sectional area. From Figure 15, it is observed that the gradient gradually decreased from 0 MPa, and reached to inflection point between 0.25 MPa and 0.275 MPa. After reaching to inflection point, the gradient increased from 0.275 MPa to 0.37 MPa. From the aforementioned result of the internal pressure of the tube, the inflection point of the internal pressure change was observed at the jet pressure of 0.25 MPa (Figure 12). Thus, it is observed that the inflection point of the gradient agrees with the inflection point of the internal pressure. Therefore, there is a possibility that jet pressure applicable to blood pressure measurement can be estimated from the gradient change of the cross-sectional area.

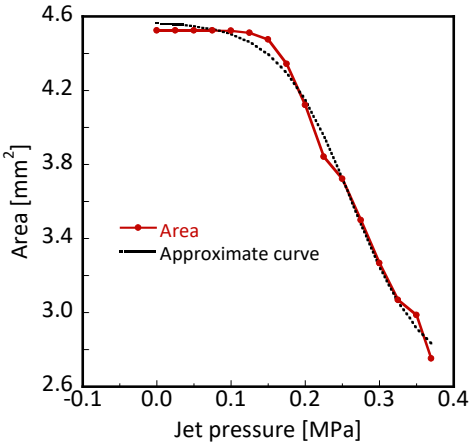

Fig. 14. Relationship between jet pressure and cross-sectional area

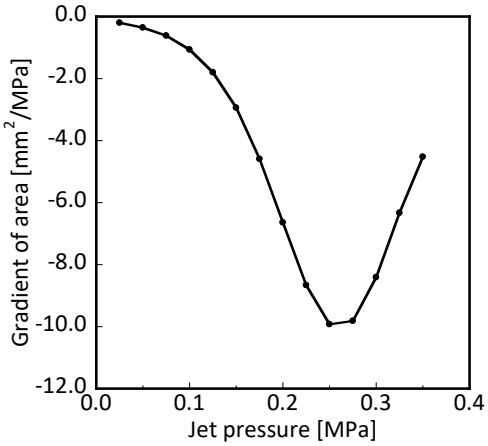

Fig. 15. Relationship between jet pressure and gradient of cross-sectional area

5. Conclusion

In this research, the novel measurement method of blood pressure is proposed which enables non-contact and continuous measurement based on the tonometry method. The experimental system is developed with elastic tube and jet flow to investigate the relationship between tube deformation and pressure of the internal liquid. The following are concluded

i. Fluctuations in the internal pressure of the elastic tube regardless of whether impinging jet flow were observed, and it is confirmed that the experimental system developed in this study can simulate the blood vessel with pulsatile flow.
ii. It is confirmed that the displacement and internal pressure of the elastic tube changed with increasing the jet pressure. Especially, the rapid increase of internal pressure was observed when the jet pressure was set to higher than 0.25 MPa. It is considered that the jet pressure must be lower than the pressure because of concern about changes in actual blood pressure.
iii. When the internal pressure increases rapidly, the gradient of the cross-sectional area of the tube with the jet pressure reached to inflection point. Therefore, there is a possibility that jet pressure applicable to blood pressure measurement can be estimated from the gradient change of the cross-sectional area.

In the future, the pressure distribution at the area where the jet flow impinges on the tube needs to be investigated in detail, and the relationship between deformation and internal pressure of the elastic tube when the jet flow is continuously targeted also needs to be elucidated.

Acknowledgment
The authors would like to thank Mr. Sho Oe, the student (National Institute of Technology, Kitakyushu College) and Mr. Kenji Arii (Kyushu Institute of Technology), the master's student, for technical assistance with the experiments. A part of this work was supported by the Grant for graduate school student working on collaborative research work with National Collage of Technology from Kyushu Institute of Technology 2022, and Research and Development Project Support Project: Seeds Creation and Practicality Verification 2022, FAIS (Kitakyushu Foundation for the Advancement of Industry, Science and Technology).

References

[1] Melville, Sarah, Robert Teskey, Shona Philip, Jeremy A. Simpson, Sohrab Lutchmedial, and Keith R. Brunt. "A comparison and calibration of a wrist-worn blood pressure monitor for patient management: assessing the reliability of innovative blood pressure devices." *Journal of Medical Internet Research* 20, no. 4 (2018): e111. https://doi.org/10.2196/jmir.8009

[2] Sharman, James E., Isabella Tan, George S. Stergiou, Carolina Lombardi, Francesca Saladini, Mark Butlin, Raj Padwal et al. "Automated 'oscillometric'blood pressure measuring devices: how they work and what they measure." *Journal of Human Hypertension* 37, no. 2 (2023): 93-100. https://doi.org/10.1038/s41371-022-00693-x

[3] Jilek, Jiri, and Teiichiro Fukushima. "Blood flow under wrist cuff, in hand alters oscillometric waveforms during blood pressure measurement." *Biomedical Instrumentation & Technology* 41, no. 3 (2007): 238-243. https://doi.org/10.2345/0899-8205(2007)41[238:BFUWCI]2.0.CO;2

[4] Lee, Bomi, Jae-Hak Jeong, Junki Hong, and Yong-Hwa Park. "Correlation analysis of human upper arm parameters to oscillometric signal in automatic blood pressure measurement." *Scientific Reports* 12, no. 1 (2022): 19763. https://doi.org/10.1038/s41598-022-24264-9

[5] Tamura, Toshiyo. "Cuffless blood pressure monitors: Principles, standards and approval for medical use." *IEICE Transactions on Communications* 104, no. 6 (2021): 580-586. https://doi.org/10.1587/transcom.2020HMI0002

[6] Tomitani, Naoko, Satoshi Hoshide, and Kazuomi Kario. "Novel blood pressure monitoring methods: perspectives for achieving "perfect 24-h blood pressure management"." *Hypertension Research* 46, no. 8 (2023): 2051-2053. https://doi.org/10.1038/s41440-023-01329-4

[7] Zheng, Dingchang, Luigi Yuri Di Marco, and Alan Murray. "Effect of respiration on Korotkoff sounds and oscillometric cuff pressure pulses during blood pressure measurement." *Medical & Biological Engineering & Computing* 52 (2014): 467-473. https://doi.org/10.1007/s11517-014-1150-1

[8] Ankishan, H., Fikret Ari, Haydar Celik, Blaise B. Frederick, Lia M. Hocke, Sinem Burcu Erdogan, and Mehmet Altay Unal. "A new system for cuffless blood pressure measurement." *Applied Acoustics* 212 (2023): 109615. https://doi.org/10.1016/j.apacoust.2023.109615

[9] Xin, Qin, and Jianping Wu. "A novel wearable device for continuous, non-invasion blood pressure measurement." *Computational Biology and Chemistry* 69 (2017): 134-137. https://doi.org/10.1016/j.compbiolchem.2017.04.011

[10] Xing, Xiaoman, Zhimin Ma, Mingyou Zhang, Ying Zhou, Wenfei Dong, and Mingxuan Song. "An unobtrusive and calibration-free blood pressure estimation method using photoplethysmography and biometrics." *Scientific Reports* 9, no. 1 (2019): 8611. https://doi.org/10.1038/s41598-019-45175-2

[11] Finnegan, Eoin, Shaun Davidson, Mirae Harford, Peter Watkinson, Lionel Tarassenko, and Mauricio Villarroel. "Features from the photoplethysmogram and the electrocardiogram for estimating changes in blood pressure." *Scientific Reports* 13, no. 1 (2023): 986. https://doi.org/10.1038/s41598-022-27170-2

[12] Li, Jian, Huiling Jia, Jingkun Zhou, Xingcan Huang, Long Xu, Shengxin Jia, Zhan Gao et al. "Thin, soft, wearable system for continuous wireless monitoring of artery blood pressure." *Nature Communications* 14, no. 1 (2023): 5009. https://doi.org/10.1038/s41467-023-40763-3

[13] Hahnen, Christina, Cecilia G. Freeman, Nilanjan Haldar, Jacquelyn N. Hamati, Dylan M. Bard, Vignesh Murali, Geno J. Merli, Jeffrey I. Joseph, and Noud van Helmond. "Accuracy of vital signs measurements by a smartwatch and a portable health device: validation study." *JMIR mHealth and uHealth* 8, no. 2 (2020): e16811. https://doi.org/10.2196/16811

[14] Moon, Joon Ho, Myung-Kyun Kang, Chang-Eun Choi, Jeonghee Min, Hae-Young Lee, and Soo Lim. "Validation of a wearable cuff-less wristwatch-type blood pressure monitoring device." *Scientific Reports* 10, no. 1 (2020): 19015. https://doi.org/10.1038/s41598-020-75892-y

[15] Jeong, In Cheol, and Joseph Finkelstein. "Introducing contactless blood pressure assessment using a high speed video camera." *Journal of Medical Systems* 40 (2016): 1-10. https://doi.org/10.1007/s10916-016-0439-z

[16] Kato, Yuki, Shunsuke Yoshimoto, Sebutaka Imura, Shingo Yamashita, Toshihiko Kostard, and Riki Oshiro. "A Fundamental Study on Non-invasive Simultaneous Measurement of Pressure Pulse Wave and Blood Flow for Circulation Dynamics Analysis." *Transactions of Japanese Society for Medical and Biological Engineering* 54, no. 2 (2016): 66-75.

[17] Meidert, Agnes S., Wolfgang Huber, Alexander Hapfelmeier, Miriam Schöfthaler, Johannes N. Müller, Nicolas Langwieser, Julia Y. Wagner, Roland M. Schmid, and Bernd Saugel. "Evaluation of the radial artery applanation tonometry technology for continuous noninvasive blood pressure monitoring compared with central aortic blood pressure measurements in patients with multiple organ dysfunction syndrome." *Journal of Critical Care* 28, no. 6 (2013): 908-912. https://doi.org/10.1016/j.jcrc.2013.06.012

[18] Cheng, H., S. Lang, C. Tufanaru, and A. Pearson. "Measurement accuracy of non-invasively obtained central blood pressure by applanation tonometry tonometry: a systematic review and meta-analysis." *International Journal of Cardiology* 167, no. 5 (2013): 1867-1876. https://doi.org/10.1016/j.ijcard.2012.04.155

[19] Salvi, Paolo, Andrea Grillo, and Gianfranco Parati. "Noninvasive estimation of central blood pressure and analysis of pulse waves by applanation tonometry." *Hypertension Research* 38, no. 10 (2015): 646-648. https://doi.org/10.1038/hr.2015.78

[20] Langwieser, Nicolas, Luisa Prechtl, Agnes S. Meidert, Alexander Hapfelmeier, Christian Bradaric, Tareq Ibrahim, Karl-Ludwig Laugwitz, Roland M. Schmid, Julia Y. Wagner, and Bernd Saugel. "Radial artery applanation tonometry for continuous noninvasive arterial blood pressure monitoring in the cardiac intensive care unit." *Clinical Research in Cardiology* 104 (2015): 518-524. https://doi.org/10.1007/s00392-015-0816-5